On the Effect of Donor Strength on the Photoluminescence Performance in Mono-substituted *N*-Donor Triarylmethyl Radicals

Mona E. Arnold,[1] Lars Roß,[2] Philipp Thielert,[3] Francisca de Almeida Neno Bartley,[2] Julia Zolg,[1] Florian Bartsch,[2] Ludwig A. Kibler,[4] Sabine Richert,[3] Christoph Bannwarth,[2]* and Alexander J.C. Kuehne[1]*

[1]Institute of Organic and Macromolecular Chemistry, Ulm University, Albert-Einstein-Allee 11, 89081 Ulm, Germany.
[2]Institute of Physical Chemistry, RWTH Aachen University, Melatener Str. 20, 52074 Aachen, Germany.
[3]Institute of Physical Chemistry, University of Freiburg, Albertstraße 21, 79104 Freiburg, Germany.
[4]Institute of Electrochemistry, Ulm University, Albert-Einstein-Allee 47, 89081 Ulm, Germany.

Abstract

The functionalization of light-emitting triarylmethyl radicals with electron donating moieties can significantly increase their photoluminescence quantum yield ϕ. As luminophores in light-emitting diodes, such open-shell radicals can be used to overcome the problem of spin-statistics inherent to conventional closed-shell emitters. However, so far the functionalization of triarylmethyl radicals with donors of varying strength has been limited by the restricted reactivity of the triarylmethyl radical, constraining optimization of performance to empirical trial and error approaches. Here, we make use of the reliable reactivity of *N*-heterocyclic donors in radical-mediated aromatic substitutions, allowing us to systematically investigate the effect of donor strength on the emission characteristics of triarylmethyl radicals. As a single descriptor proxy to the donor strength, we employ the ionization energy *IE* of the donor moiety determined by density functional theory calculations. A systematic bathochromic shift of the emission wavelength λ_{max} is observed for increasing donor strength, while maximum ϕ values are obtained for medium-strength donors. We rationalize these effects with a simple model based on the Marcus theory supported by quantum chemical calculations and electron paramagnetic resonance. This allows us to understand the effect of the donor strength on both λ_{max} and ϕ, enabling the design of improved light-emitting radicals in the future.

Introduction

Donor-functionalized open-shell tris(2,4,6-trichlorophenyl)methyl (TTM) radicals have emerged as a powerful class of stable and highly efficient doublet emitters.[1] A large variety of TTM derivatives, mainly functionalized by carbazole (Cz) moieties, has been reported, with fluorescence covering the orange to near-infrared region of the spectrum.[2–4] TTM-Cz radicals with high photoluminescence quantum yield (ϕ) have been employed in electroluminescent devices (OLEDs), showing high efficiency beyond the spin-statistical limitations of conventional closed-shell emitters.[5] The substitution of TTM with Cz-type electron donors evokes charge transfer (CT) from the donor to the trityl site after excitation, leading to red-shifted emission in comparison to the unsubstituted TTM radical.[4] Surprisingly, ϕ of these mono-substituted TTM radicals varies greatly; from a few percent to almost unity in pyridoindole functionalized TTM radicals.[3,4,6] For TTM-Cz and some pyroindole derivatives, coupling of the CT excited state with ground or locally excited states has been discussed to improve the radiative decay rate; however, the coupling mechanism remains elusive and a predictive theory is absent to date.[6–8] A fundamental understanding of the factors determining

the shift in the fluorescence maximum λ_{max} and the variability in ϕ would be desirable to enable the rational design of radicals with emission properties specifically tailored to the respective applications. Studies of donor-substituted TTM radicals have shown that their emission properties depend on the nature of the CT excited state.[4] However, to date, there is no comparative study that sheds light on the influence of the donor strength to improve ϕ and its effect on the emission wavelength.

Here, we address the fragmented data situation and compare a variety of *N*-heterocyclic donor- and acceptor-functionalized TTM radicals with regard to their emission properties.[2–4,6,8–15] We compare reported molecules and close some gaps by synthesizing unprecedented donor-substituted TTM radicals. For the comparison, we consider reported λ_{max} and ϕ values that are comparable with respect to the type of solvent used and the method of property determination employed. All of the newly synthesized molecules are accessible *via* the established radical-mediated aromatic substitution approach and characterized respecting the same criteria as for the reported data.[2,3] The ionization energy (*IE*) of the donor has previously been suggested to influence the excited state energy.[8] Here, we employ the *IE* as a proxy for the donor strength of the *N*-substituents, which we determine for all molecules under consideration (previously reported and newly synthesized) using density functional theory (DFT) calculations. We find a systematic dependence of λ_{max} with increasing *IE* and a deteriorating ϕ for strong and very weak donors, while the best ϕ is achieved in molecules with medium donor strength.

Results and Discussion

Selection of N-Donor Funtionalized TTMs and Their Emission Behavior

We select a variety of TTM radicals functionalized with *N*-heterocyclic donors – mostly substituted carbazoles – from the literature.[2–4,6,8–17] We group the molecules into four different categories according to the structure of the donor: (i) varying carbazole ring reductions and extensions, (ii, iii) different carbazole substitutions (either 2,7- or 3,6-), and (iv) *N*-heterocyclic moieties other than carbazole (see Figure 1). To obtain a measure for the electron-donating quality of the respective substituents, we employ DFT calculations on the PBE0/6-31+G(d) level of theory (and, for the donors of **22** and **23,** the LANL2DZ basis set because of the heavy iodide substituents).[18–22] The *IE* is obtained as the vertical difference in total energy of the neutral and cationic species, while the geometry, optimized for the neutral compounds, is unchanged upon ionization (see Figure 1).

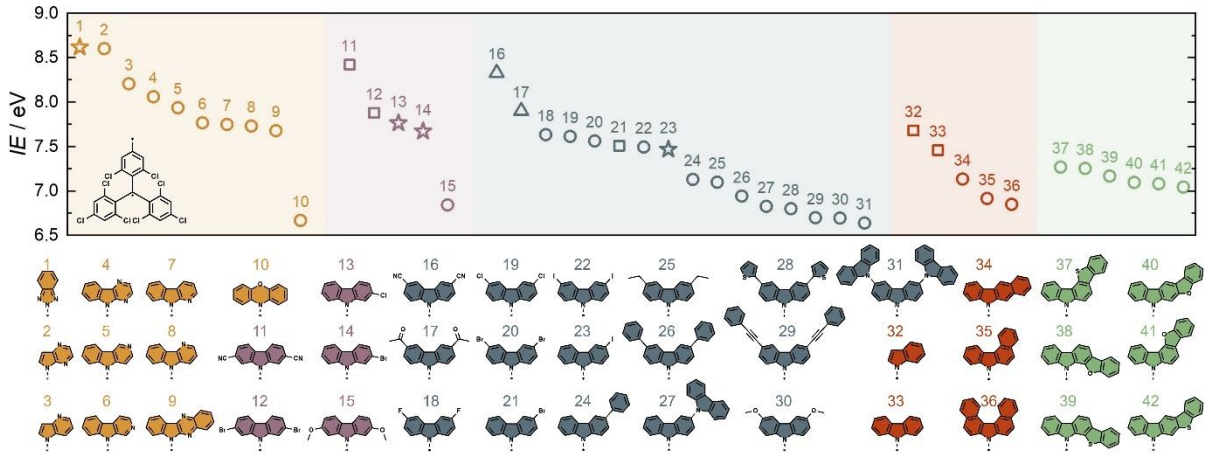

Figure 1: *Structures and ionization energies (IE) of various substituents attached to TTM.*[2–4,6,8–16] *These are computed for the individual molecules (saturated with hydrogen) at the PBE0/6-31+G(d) level (LANL2DZ basis set for the donors of* ***22*** *and* ***23****).*[18–22] *Circles, squares, and triangles represent molecules taken from the literature; new compounds are indicated by stars. Circles: Literature-known radicals characterized from cyclohexane solutions.*[2–4,6,8–14,17] *Triangles: Radicals characterized in toluene solutions.*[3] *Squares: Reported radicals for which* ϕ *is newly determined in cyclohexane solutions.*[2,11,12,15] *Stars: New compounds characterized in cyclohexane solutions.*

Experimental *IE* values are available for some of the donor molecules discussed here and our calculated *IE* values are in good agreement with these reported values. In the literature, the *IE* for Cz varies between 7.2 and 7.68 eV, while we calculate 7.4 eV.[23–30] Employing an inexpensive basis set allows us to screen a broad variety of potential substituents quickly and at low computational cost. We perform these calculations for the respective substituents of all radical structures drawn from the literature and find that there are some apparent gaps, which we fill by synthesizing and calculating four unprecedented functionalized TTM radicals, namely benzotriazole- (Bta; **1**), 2-chlorocarbazole- (**13**), 2-bromocarbazole- (**14**), and 3-iodocarbazole- (**23**) (indicated by stars in Figure 1, see Supporting Information for synthetic procedures). We determine ϕ and λ_{max} in solution by recording photoluminescence spectra of these new compounds, and we plot the data together with λ_{max} and ϕ reported for the respective donor-functionalized radicals extracted from the literature (see Figure 1). The emission of *N*-donor-functionalized TTM radicals typically occurs from a CT excited state.[2,4,15] The CT state is stabilized in polar solvents, which leads to a decrease in ϕ, while non-polar solvents yield much higher ϕ.[2] Therefore, we decide to compare the emission of the *N*-donor-functionalized TTMs in cyclohexane (or toluene solution for two compounds in lieu of data in cyclohexane, see Figure 1). The emission maxima of all compared compounds vary largely between λ_{max} = 583 nm and 728 nm.[4] When plotting the reported and measured λ_{max} of the respective *N*-donor-functionalized TTM radicals against the *IE*, we observe a non-linear increase of λ_{max} with increasing donor strength (see Figure 2a; the black line is a guide to the eye). For strong donors, the spread of the λ_{max} values increases when compared to the medium strength and weak donors. This effect may be rooted in the broader spectra that are typically observed for emission from clear CT states. At the low donor strength end of the curve, compound **1** (TTM-Bta) seems to deviate most strongly from the general trend. At this point, the donor strength of Bta might be too weak to evoke a CT excited state (cf. Figure 2 and Table S1 in the Supporting Information). The photoluminescence of TTM-Bta (**1**) is independent of the solvent polarity, likely indicating emission from a locally excited (LE) state (see Figure S3 and Figure S5 in the Supporting Information). The increased aromatic delocalization of such an LE state, could

explain the greater-than-expected λ_{max}. However, the ϕ of TTM-Bta (**1**) is low, indicating that LE states are unfavourable in TTM-based radical emitters.

The determination of ϕ of dissolved emitters can be performed either by an absolute method using an integrating sphere or by a relative method where a series of degressively diluted sample solutions is measured against a reference emitter of known ϕ. Altogether, the determination of ϕ is prone to errors.[31–34] In the literature, both absolute and relative methods have been employed for the determination of ϕ for *N*-donor functionalized TTM radicals. When we plot ϕ against *IE*, we observe that the data describe a bell-shaped curve, showing poor ϕ for weak and strong donors, and high ϕ for medium-strength donors (see Figure 2b).

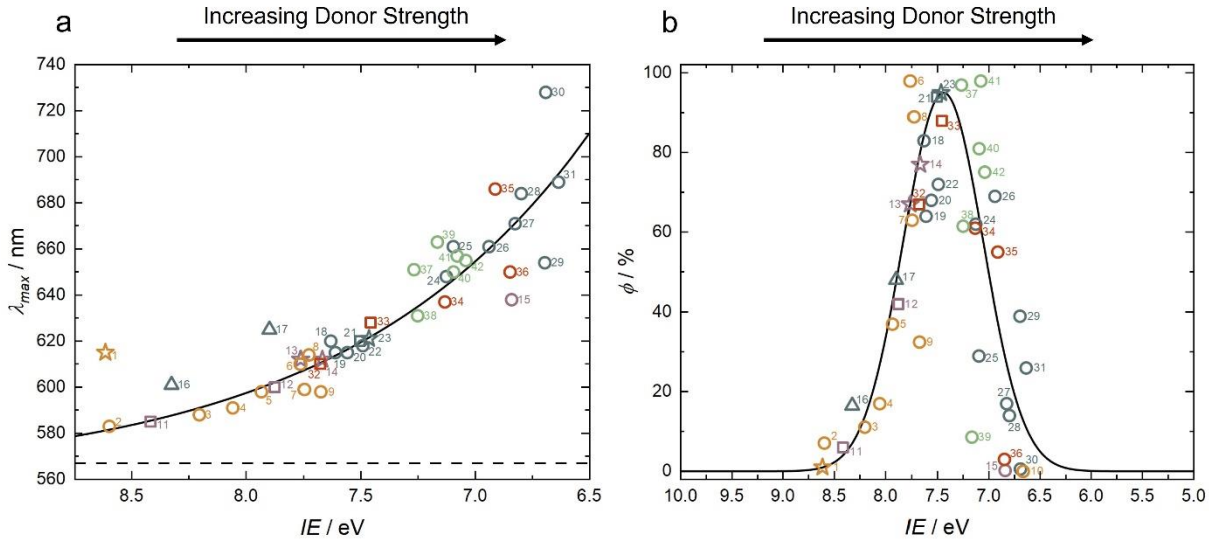

Figure 2: *(a) Emission wavelength λ_{max} and (b) fluorescence quantum yield ϕ of the TTM derivatives in cyclohexane solution as a function of the ionization energies (IE) of the respective substituents.*[2–4,6,8–17] *The solid line in Figure 2 (a), approaching λ_{max} of TTM (567 nm) in cyclohexane (dashed line) and the Gauss curve (black solid line in Figure 2 (b)) are guides to the eye. Data points marked by triangles are for solutions of the respective radicals in toluene.*[3]

While most data follow the bell-shaped curve, for compound **21** no ϕ has been reported and for radicals **32** and **33** disparate values are found in the literature.[2,4,8,13,15–17] Therefore, we synthesize these compounds, determine their ϕ using the absolute method in an integrating sphere and include the new data in Figure 2b (indicated by square-shaped datapoints). For compound **32** we amend the reported ϕ to 68 %; by contrast, compound **33** (TTM-Cz) delivered $\phi = 88$ %, which is higher than reported previously.[35] However, recent investigations also point towards higher ϕ for TTM-Cz, which is why we chose to continue using our results in this study (see Figure 2b).[16]

Excited State Characteristics

To elucidate whether the excited state character gives information about the above-described trends in λ_{max} and ϕ, we select radicals at the bottom of the bell-shaped curve with low ϕ from the left and right branch of the curve (**2** & **10**), and one molecule with very high ϕ (**33**). We optimize their ground (D_0) with Kohn-Sham DFT and first excited state (D_1) geometries using ΔSCF initial maximum overlap method ((IMOM-), both at the PBE0-D3(BJ)/def2-SVP

level.[36–45] We determine the canonical orbitals involved in the transition using (ΔSCF -)PBE0-D3(BJ)/def2-SVP (see Figure 3). These are the highest occupied spin-down orbitals in D_0 and D_1. The D_1 excited state in TTM-Cz (**33**) results from an intramolecular charge transfer (ICT) from the carbazole donor to the TTM acceptor moiety,[2,4,46] as can be deduced from the involved orbitals (see Figure 3c). With increasing *IE*, the strength of the *N*-donor decreases, entailing a pronounced LE state of low ϕ (cf. (**2**) in Figures 2 and 3a). The involved orbitals of TTM-Bta (**1**) also exhibit a clear LE state as expected from the polarity independent photoluminescence discussed above, corroborating our hypothesis that the enlarged π-system evokes the bathochromic shift in λ_{max} (cf. Figure S3 and Figure S5 in the Supporting Information). The orbitals of radicals with strong donors (**10**) exhibit an even more pronounced CT state than TTM-Cz (**33**), especially when considering the distribution of the hole in the D_0 geometry (see Figure 3c). Apparently, the variation of the *IE* of the donor influences the excited state character of the TTM derivative.

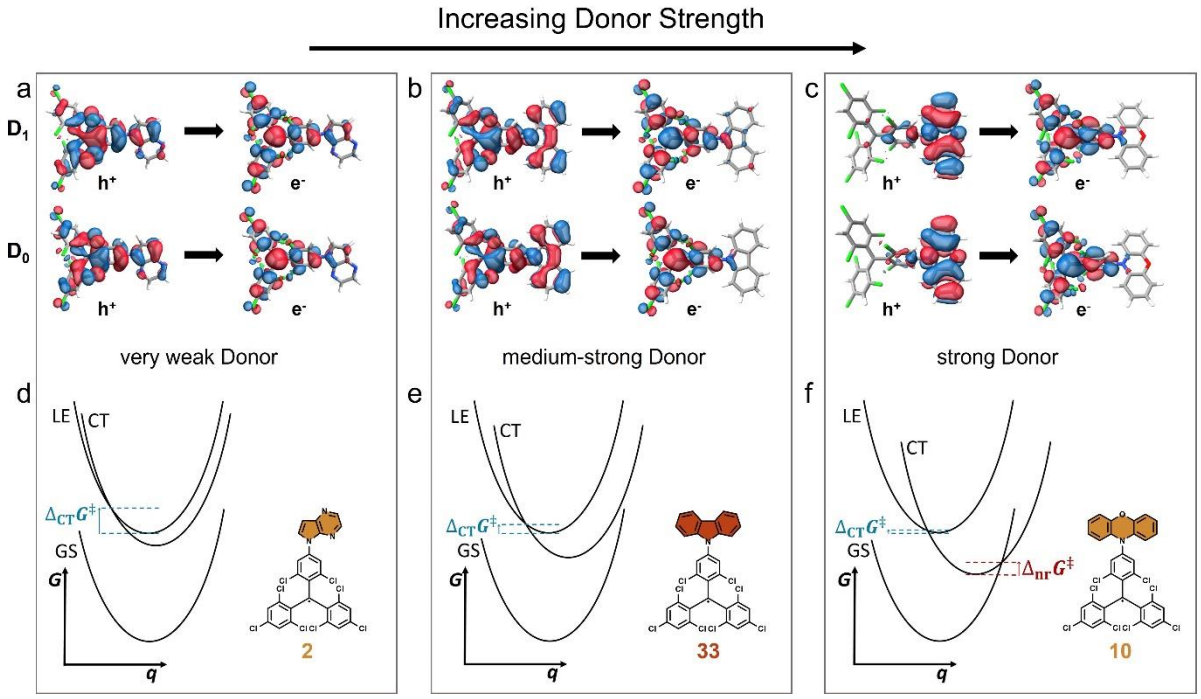

Figure 3: *(a – c) Hole (h^+) and particle (e^-) molecular orbitals for the selected radicals in their ground (D_0) and excited state (D_1) geometry calculated on the (IMOM-)PBE0-D3(BJ)/def2-SVP level. Functionalization with a very weak donor leads to LE behavior (**2**) as for TTM, while donors evoke CT to the TTM moiety (**33**, **10**). 3-state model for LE, CT, and GS in selected derivatives carrying a very weak donor (**2**, d), a medium-strength donor (**33**, e), and a strong donor (**10**, f).*[8] *When increasing the donor strength, the CT curve is lowered in its free energy and displaced on the charge transfer coordinate with respect to the LE, qualitatively explaining the red-shifted emission.*

According to the quantum chemical calculations for molecule **33**, at the ΔSCF-DFT level the relaxation of the excited state to the D_1 minimum proceeds *via* a barrierless rotation around the donor-TTM bond with no state crossing involved.[36–45] Involvement of two separate adiabatic states that represent the LE and CT state, was also ruled out by means of TD-DFT calculations. Hence, for medium-strength donors, we assume almost instantaneous relaxation of the locally excited D_1 state (found vertically at the D_0 minimum) to a relaxed state with more pronounced CT character. For strong donors (like in molecule **10**), we only find an excited state D_1 with distinct CT character, while for weak donors we only find an LE D_1 state, as shown for radicals

2 and **1** (cf. Figure 3a,c and Figure S5). Orbital plots for all investigated systems can be found in the Supporting Information (see Figure S8).

A Simple 3-State Model Treated in the Context of Marcus Theory

Encouraged by these results, we proceed to rationalize the emission properties for the wide spectrum of *N*-donors with different strength. Given that two different excited-state characters (LE and CT) exist, we also expect two different non-radiative decay mechanisms to return to the ground state. Our rationalization is achieved by employing a simple 3-state model involving LE, CT, and ground state (GS). The 3-state model has previously been suggested for TTM-based radicals;[8] here we apply Marcus theory for ICT to this model. The key aspects of the model are outlined in the following:

We assume that, after photo-excitation, an LE state is populated, which can undergo ICT to a CT state. Moreover, we hypothesize that, in the absence of ICT, the LE state itself exhibits non-radiative relaxation pathways to the GS. This hypothesis is corroborated by the low ϕ of TTM without donor functionalization (λ_{max} = 567 nm, ϕ = 2 %). In our Marcus theory treatment, weak donors, like in radical **2**, lead to a large energy barrier between the LE minimum and the transition state to the CT state ($\Delta_{CT}G^{\ddagger}$), rendering the transition from the LE state to the CT state unfavorable (see Figure 3d). Therefore, we observe only weak emission for radicals functionalized with weak donors. As expected, the emission energy is close to that of non-functionalized TTM (λ_{max} = 567 nm, see Figure 2a). When we increase the strength of the donor, the free energy of the CT state decreases. In addition, the CT character will become more pronounced, leading to a shift along the electron transfer coordinate *q* (see Figure 3e). Both effects decrease the free energy difference between CT and GS, rationalizing the bathochromic shift (red-shift) of the emission wavelength maximum. Radicals carrying medium-strength donors, like TTM-Cz (**33**), possess a much smaller $\Delta_{CT}G^{\ddagger}$ barrier enabling fast ICT to the CT state and efficient emission from this state (cf. Figure 3e).

For strong donors, like in radical **10**, the CT state will be further stabilized and shifted with respect to the LE state, resulting in very low values for $\Delta_{CT}G^{\ddagger}$. This assumption is substantiated by the orbitals of radical **10**, indicating augmented charge separation upon excitation, compared to radical **33** (see Figure 3c). However, simultaneously, a low barrier conical intersection (CI) between the CT and GS will occur, opening up a non-radiative decay pathway (see Figure 3f). This new pathway explains the drop in ϕ for decreasing *IE* (strong donors).[47,48]

Quantum Chemical Calculations on the Photophysics

To further test the applicability of our model, we determine the suspected state transition energy barriers. We want to point out that our quantum chemical calculations indicate direct excitation to a CT state for medium-strength and strong donors with no previous involvement of an LE state (see Figure 3c). This apparent discrepancy between the 3-state model and our quantum chemical calculations can be brought into agreement when considering that in our model the relaxation from the LE to the CT state is practically barrierless and fast. Likewise, for the weak

donor case, our calculations indicate no existence of CT character in the D_1 state and only LE character. In the suggested 3-state model, this would be reflected by a much larger $\Delta_{CT}G^{\ddagger}$ compared to direct relaxation to the ground state.

The energy barrier to the ground state is determined as the difference between the charge separated D_1 state minimum and the minimum energy conical intersection with the D_0 ground state. Thermodynamic corrections employing the rigid-rotor harmonic oscillator approximation ($\Delta G^{\ddagger}$) are applied as well. This $\Delta G^{\ddagger}$ is used to estimate the energy barrier of non-radiative internal conversion to the ground state $k_{\mathrm{IC}}^{\mathrm{D1}}$ (see Table 1). Since ΔSCF-DFT is not capable of determining conical intersection geometries, we determine $\Delta G^{\ddagger}$ and the radiative decay rates using FOMO-CAS(3,2)-CI-D3(BJ)[49,50] employing the def2-SV(P)[51,52] basis set in TerachemV1.9 (for details see Supporting Information).[53] The active space of 3 electrons in 2 active orbitals (singly occupied molecular orbital (SOMO) and doubly occupied molecular orbital (HDMO)) is chosen because these are sufficient to reproduce the emission energies utilizing the ΔSCF approach with PBE0-D3(BJ)/def2-SVP (see Figure S7).[36–45] Here the transition of the spin-down electron from HDMO to SOMO matches the experimentally observed emission energy (see also Supporting Information for further clarification).

To obtain insight into the radiative and non-radiative relaxation scenarios with varying *IE*, we determine the rate constants. First, $k_{\mathrm{r}}^{\mathrm{D1}}$ is determined using the Einstein coefficient A_{21}.[36] The emission energy ΔE is calculated utilizing afore mentioned ΔSCF theory level using PBE0-D3(BJ)/def2-SVP. The oscillator strength f_{12} is computed by the FOMO-CAS(3,2)-CI-D3(BJ) at the respective D_1 minimum.(for details, see Supporting Information).
Secondly, the non-radiative rate constant $k_{\mathrm{IC}}^{\mathrm{D_1}}$ is estimated by using non-adiabatic transition state theory the nonadiabatic coupling (NAC) elements are also computed using FOMO-CAS(3,2)-CI.[54]

Table 1: *Computational results on f_{12}, ΔE, $|NAC|^2$ and $\Delta G^{\ddagger}$. The resulting rate constants for radiative relaxation and non-radiative internal conversion (IC) are also given. For computational details, see the Supporting Information.*

Molecule	ϕ^{exp} [%]	f_{12}	ΔE [eV]	$\lvert\mathrm{NAC}\rvert^2$	$\Delta G^{\ddagger}$ [eV]	$k_{\mathrm{r}}^{\mathrm{D1}}$ [s^{-1}]	$k_{\mathrm{IC}}^{\mathrm{D1}}$ [s^{-1}]	ϕ^{exp} [%]
TTM	2	$2.80 \cdot 10^{-1}$	2.09	$1.49 \cdot 10^{-3}$	1.41	$5.30 \cdot 10^{7}$	$9.04 \cdot 10^{2}$	100
1	1	$5.00 \cdot 10^{-1}$	2.03	$1.51 \cdot 10^{-3}$	1.36	$8.97 \cdot 10^{7}$	$8.99 \cdot 10^{3}$	99.9
2	7,1	$3.64 \cdot 10^{-1}$	2.02	$9.07 \cdot 10^{-3}$	1.50	$6.45 \cdot 10^{7}$	$1.65 \cdot 10^{2}$	100
33	88	$7.43 \cdot 10^{-2}$	1.99	$2.47 \cdot 10^{-3}$	1.24	$1.27 \cdot 10^{7}$	$1.26 \cdot 10^{6}$	91.0
10	0	$0.22 \cdot 10^{-2}$	1.45	$2.90 \cdot 10^{-4}$	0.80	$2.00 \cdot 10^{5}$	$4.57 \cdot 10^{12}$	0.0

For decreasing *IE*, the energy barrier for non-radiative internal conversion ΔE and f_{12} decrease (see Table 1). These results are in line with our experimental observations (cf. Figure 2a). Our computational study indicates two trends for strong and medium donors with increasing donor strength: $k_{\mathrm{r}}^{\mathrm{D_1}}$ decreases only slightly, while $k_{\mathrm{IC}}^{\mathrm{D_1}}$ increases drastically. This increase in $k_{\mathrm{IC}}^{\mathrm{D_1}}$ explains why we observe a low ϕ for strong donors.

Computationally, radicals carrying very weak donors (like molecule **2**) or even very weak acceptors (like molecule **1**) apparently cannot be simulated with this approach, as they show much larger quantum yields, in contrast to the experimental observation. This needs to be investigated in further detail. We expect that excited states of higher spin multiplicity (quartets) are involved in the relaxation process. For example, in TTM-Bta (**1**), electron paramagnetic resonance (EPR) analysis indicates the population of a quartet state after photo-excitation. This indicates a spin-forbidden non-radiative decay pathway and could explain its low ϕ (cf. Figure 2 and Figure S6 in the Supporting Information). As a result, weak donors and acceptors require further investigation to understand their poor emission properties; however, this is not the aim of the present study.

Relaxation Rates in the 3-State Model of Donor-functionalized TTM Radicals

The results obtained from the quantum chemical calculations together with the simple 3-state model allow us to develop a phenomenological treatment of the experimental observations.[8] The rate constant of ICT ($k_{\mathrm{LE-CT}}$) plays a keyrole in rationalizing the influence of the *IE* on ϕ. As described above, ϕ depends on the rate constants of radiative and non-radiative decay from the LE and the CT states, respectively. A steady-state approximation for the population of the excited states leads to an expression of ϕ as a function of the relevant rate constants *k* (see Supporting Information).

$$\phi = k_{\mathrm{r}}^{\mathrm{LE}} \cdot \frac{1}{k_{\mathrm{r}}^{\mathrm{LE}}+k_{\mathrm{nr}}^{\mathrm{LE}}+k_{\mathrm{LE-CT}}} + k_{\mathrm{r}}^{\mathrm{CT}} \cdot \frac{k_{\mathrm{LE-CT}}}{(k_{\mathrm{LE-CT}}+k_{\mathrm{r}}^{\mathrm{LE}}+k_{\mathrm{nr}}^{\mathrm{LE}})(k_{\mathrm{r}}^{\mathrm{CT}}+k_{\mathrm{nr}}^{\mathrm{CT}})} \qquad \text{(Eq. 1)}$$

In the absence of ICT ($k_{\mathrm{LE-CT}} = 0$), this expression simplifies to $\phi = \frac{k_{\mathrm{r}}^{\mathrm{LE}}}{k_{\mathrm{r}}^{\mathrm{LE}}+k_{\mathrm{nr}}^{\mathrm{LE}}}$, which is around 2 % for TTM in cyclohexane, signifying that $k_{\mathrm{nr}}^{\mathrm{LE}}$ is about 50 times larger than $k_{\mathrm{r}}^{\mathrm{LE}}$. An increase in donor strength (by lowering IE of the donor moiety systematically) is found to be crucial for tuning of $k_{\mathrm{LE-CT}}$. Maximum enhancement of ϕ is expected for large $k_{\mathrm{LE-CT}}$ with a limiting value of $\phi = \frac{k_{\mathrm{r}}^{\mathrm{CT}}}{k_{\mathrm{r}}^{\mathrm{CT}}+k_{\mathrm{nr}}^{\mathrm{CT}}}$. Accordingly, donor-functionalized TTM radicals with strong emission require improved ICT but also the prevention of non-radiative decay of the CT excited state to minimize $k_{\mathrm{nr}}^{\mathrm{CT}}$. As established above, strong donors may facilitate non-radiative decay, due to efficient crossing from D_1 to D_0 *via* a conical intersection.

Using these conditions together with the above-delineated 3-state Marcus theory for ICT, we can elaborate on the dependence of $k_{\mathrm{LE-CT}}$ and $k_{\mathrm{nr}}^{\mathrm{CT}}$ on *IE* (see Supporting Information). Both $k_{\mathrm{LE-CT}}$ and $k_{\mathrm{nr}}^{\mathrm{CT}}$ represent normal distributions (see Supporting Information).

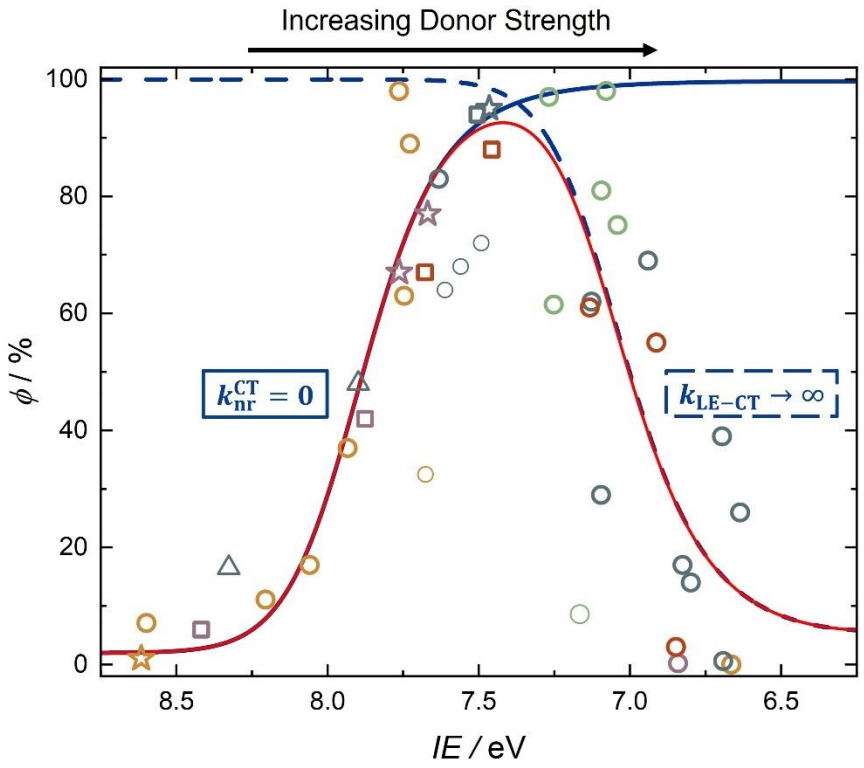

Figure 4: *Photoluminescence quantum yield ϕ as a function of the ionization energy of the donor moiety attached to TTM with* $\frac{k_{nr}^{LE}}{k_{r}^{LE}} = 50$. In the absence of non-radiative decay of the CT state, *ϕ is enhanced for stronger donors by a systematic increase in the rate constants k_{LE-CT} at lower IE (blue curve). The dashed curve shows the dependence of ϕ on IE in case that non-radiative decay of the CT state is the sole deactivation process ($k_{LE-CT} \rightarrow \infty$). The red curve results from eq. 1, by plugging in the fitted parameters obtained from the blue curves (with $k_{LE-CT} \rightarrow \infty$ and $k_{nr}^{CT} = 0$, respectively). Outlying data points, marked by thin lines, are not included in the fit.*

We assume that k_{nr}^{CT} (*via* an intersection to the GS) only becomes important for $IE < 7.5$ eV (strong donors) and that the ICT rate k_{LE-CT} (*via* a transition state between LE and CT) only becomes important for $IE \geq 7.5$ eV (weak donors). Therefore, we set $k_{nr}^{CT} = 0$ and fit the parameters of k_{LE-CT} (in Eq. 1) to the low donor strength branch of the experimental data (ϕ versus $IE \geq 7.5$ eV), leading to the solid blue curve in Figure 4. For rationalizing the complete set of experimental data, the impact of IE on k_{nr}^{CT} for high donor strengths $IE < 7.5$ eV has to be considered as well. Therefore, we set $k_{LE-CT} \rightarrow \infty$ to account for the barrier-free/direct population of the CT state (as indicated by our calculations for compound **10**) and we fit the parameters of k_{nr}^{CT} (in Eq. 1) to the strong donor branch (ϕ versus $IE < 7.5$ eV). The resulting dashed blue curve illustrates the contribution of non-radiative decay of the CT state (e.g., *via* a conical intersection to the GS) to ϕ for the hypothetical case of the absence of other deactivation processes (see Figure 4). Now, with the obtained parameters for k_{LE-CT} and k_{nr}^{CT}, we can employ Eq. 1 to describe the bell-shaped curve for *IE* versus ϕ.

Conclusions

We have introduced a simple strategy for the prediction of λ_{max} and ϕ of a variety of *N*-heterocycle-functionalized TTM derivatives. As the essential factor determining these properties, we identify the donor strength of the respective substituent that is represented by its

ionization energy *IE*, which is easily calculated by density functional theory (DFT). Our phenomenological analysis using a 3-state model for LE-type and CT-type excited states and the ground state in the context of Marcus theory elucidates the influence of $k_{\mathrm{LE-CT}}$ and $k_{\mathrm{nr}}^{\mathrm{CT}}$ on the electronic properties of the donor, as expressed by the *IE* as a simple descriptor. This model is supported by quantum chemical calculations and observations from EPR spectroscopy.
The general understanding of the competitive relaxation processes in donor-functionalized TTMs enables a prediction of the optical properties of further derivatives prior to their synthesis. Such knowledge allows the rational design of efficient open-shell emitters with desired fluorescence properties.

Author Information

Corresponding Author
* e-mail: alexander.kuehne@uni-ulm.de
* e-mail: bannwarth@pc.rwth-aachen.de

Acknowledgements

This work was supported by the Deutsche Forschungsgemeinschaft (DFG, German Research Foundation) – Project numbers 500226157 (A.J.C.K. and C.B.) and 417643975 (S.R.). The authors acknowledge support by the state of Baden-Württemberg through bwHPC and the DFG through grant number INST 40/575-1 FUGG (JUSTUS 2 cluster). C. B. acknowledges funding by the Federal Ministry of Education and Research (BMBF) and the Ministry of Culture and Science of the State of North Rhine-Westphalia (MKW) as part of TRA Matter and the Excellence Strategy of the federal and state governments. Simulations were performed with computing resources granted by RWTH Aachen University under project rwth0713. We thank Dr. Markus Lamla for performing mass spectrometry and Tobias Wasserrab for support during radical synthesis (both at Ulm University).

References

[1] A. Mizuno, R. Matsuoka, T. Mibu, T. Kusamoto, *Chem Rev* **2023**, DOI 10.1021/acs.chemrev.3c00613.

[2] V. Gamero, D. Velasco, S. Latorre, F. López-Calahorra, E. Brillas, L. Juliá, *Tetrahedron Lett* **2006**, *47*, 2305–2309.

[3] D. Velasco, S. Castellanos, M. López, F. López-Calahorra, E. Brillas, L. Juliá, *J Org Chem* **2007**, *72*, 7523–7532.

[4] L. Fajarí, R. Papoular, M. Reig, E. Brillas, J. L. Jorda, O. Vallcorba, J. Rius, D. Velasco, L. Juliá, *J Org Chem* **2014**, *79*, 1771–1777.

[5] X. Ai, E. W. Evans, S. Dong, A. J. Gillett, H. Guo, Y. Chen, T. J. H. Hele, R. H. Friend, F. Li, *Nature* **2018**, *563*, 536–540.

[6] A. Abdurahman, T. J. H. Hele, Q. Gu, J. Zhang, Q. Peng, M. Zhang, R. H. Friend, F. Li, E. W. Evans, *Nat Mater* **2020**, *19*, 1224–1229.

[7] E. Cho, V. Coropceanu, J. L. Brédas, *J Mater Chem C Mater* **2021**, *9*, 10794–10801.

[8] C. Lu, E. Cho, Z. Cui, Y. Gao, W. Cao, J. L. Brédas, V. Coropceanu, F. Li, *Advanced Materials* **2023**, *35*, DOI 10.1002/adma.202208190.

[9] M. Reig, C. Gozálvez, V. Jankauskas, V. Gaidelis, J. V. Grazulevicius, L. Fajarí, L. Juliá, D. Velasco, *Chemistry - A European Journal* **2016**, *22*, 18551–18558.

[10] S. Dong, A. Obolda, Q. Peng, Y. Zhang, S. Marder, F. Li, *Mater Chem Front* **2017**, *1*, 2132–2135.

[11] L. Chen, M. Arnold, Y. Kittel, R. Blinder, F. Jelezko, A. J. C. Kuehne, *Adv Opt Mater* **2022**, *10*, DOI 10.1002/adom.202102101.

[12] X. Bai, W. Tan, A. Abdurahman, X. Li, F. Li, *Dyes and Pigments* **2022**, *202*, 110260.

[13] K. Matsuda, R. Xiaotian, K. Nakamura, M. Furukori, T. Hosokai, K. Anraku, K. Nakao, K. Albrecht, *Chemical Communications* **2022**, DOI 10.1039/D2CC04481A.

[14] M. E. Arnold, A. J. C. Kuehne, *Dyes and Pigments* **2022**, *208*, DOI 10.1016/j.dyepig.2022.110863.

[15] M. López, D. Velasco, F. López-Calahorra, L. Juliá, *Tetrahedron Lett* **2008**, *49*, 5196–5199.

[16] K. Nakamura, K. Matsuda, X. Rui, M. Furukori, S. Miyata, T. Hosokai, K. Anraku, K. Nakao, K. Albrecht, *Faraday Discuss* **2023**, DOI 10.1039/d3fd00130j.

[17] C. Lu, E. Cho, K. Wan, C. Wu, Y. Gao, V. Coropceanu, J. L. Brédas, F. Li, *Adv Funct Mater* **2024**, DOI 10.1002/adfm.202314811.

[18] J. P. Perdew, M. Ernzerhof, K. Burke, *J Chem Phys* **1996**, *105*, 9982–9985.

[19] C. Adamo, V. Barone, *J Chem Phys* **1999**, *110*, 6158–6170.

[20] G. A. Petersson, A. Bennett, T. G. Tensfeldt, M. A. Al-Laham, W. A. Shirley, J. Mantzaris, *J Chem Phys* **1988**, *89*, 2193–2218.

[21] G. A. Petersson, M. A. Al-Laham, *J Chem Phys* **1991**, *94*, 6081–6090.

[22] W. R. Wadt, P. J. Hay, *J Chem Phys* **1985**, *82*, 284–298.

[23] L. Domelsmith, K. Houk, *NIDA Res Monograph* **1987**, *22*, 423–440.

[24] J. W. Hager, S. C. Wallace, *Anal. Chem* **1988**, *60*, 54.

[25] W. Riepe, M. Zander, *Zeitschrift für Naturforschung A* **1969**, *24*, 2017–2018.

[26] B. R. Uščić, B. Kovač, L. Klasinc, H. Güsten, *Zeitschrift für Naturforschung A* **1978**, *33*, 1006–1012.

[27] J. Hager, M. Ivanco, M. A. Smith, S. C. Wallace, *Chem Phys Lett* **1985**, *113*, 503–507.

[28] V. K. Potapov, I. E. Kardash, V. V. Sorokin, S. A. Sokolov, T. I. Evlasheva, *Khim. Vys. Energ.* **1972**, *6*, 392.

[29] U. Rapp, H. A. Staab, C. Wünsche, *Organic Mass Spectrometry* **1970**, *3*, 45–49.

[30] H. J. Haink, J. E. Adams, J. R. Huber, *Berichte der Bunsengesellschaft für physikalische Chemie* **1974**, *78*, 436–440.

[31] C. Würth, M. Grabolle, J. Pauli, M. Spieles, U. Resch-Genger, *Anal Chem* **2011**, *83*, 3431–3439.

[32] C. Würth, J. Pauli, C. Lochmann, M. Spieles, U. Resch-Genger, *Anal Chem* **2012**, *84*, 1345–1352.

[33] L. Porrès, A. Holland, L. O. Pålsson, A. P. Monkman, C. Kemp, A. Beeby, *J Fluoresc* **2006**, *16*, 267–273.

[34] F. Fries, S. Reineke, *Sci Rep* **2019**, *9*, DOI 10.1038/s41598-019-51718-4.

[35] M. Gross, F. Zhang, M. E. Arnold, P. Ravat, A. J. C. Kuehne, *Adv Opt Mater* **2023**, DOI 10.1002/adom.202301707.

[36] A. Hellman, B. Razaznejad, B. I. Lundqvist, *J Chem Phys* **2004**, *120*, 4593–4602.

[37] J. Gavnholt, T. Olsen, M. Engelund, J. Schiøtz, *Phys Rev B* **2008**, *78*, DOI 10.1103/PhysRevB.78.075441.

[38] E. Muchova, D. Hollas, D. M. P. Holland, C. Bacellar, L. Leroy, T. R. Barillot, L. Longetti, M. Coreno, M. de Simone, C. Grazioli, M. Chergui, R. A. Ingle, *Physical Chemistry Chemical Physics* **2023**, *25*, 6733–6745.

[39] A. T. B. Gilbert, N. A. Besley, P. M. W. Gill, *Journal of Physical Chemistry A* **2008**, *112*, 13164–13171.

[40] N. A. Besley, A. T. B. Gilbert, P. M. W. Gill, *J Chem Phys* **2009**, *130*, DOI 10.1063/1.3092928.

[41] G. Macetti, A. Genoni, *J Chem Theory Comput* **2021**, *17*, 4169–4182.

[42] G. M. J. Barca, A. T. B. Gilbert, P. M. W. Gill, *J Chem Phys* **2014**, *141*, DOI 10.1063/1.4896182.

[43] G. M. J. Barca, A. T. B. Gilbert, P. M. W. Gill, *J Chem Theory Comput* **2018**, *14*, 1501–1509.

[44] G. M. J. Barca, A. T. B. Gilbert, P. M. W. Gill, *J Chem Theory Comput* **2018**, *14*, 9–13.

[45] S. Seritan, C. Bannwarth, B. S. Fales, E. G. Hohenstein, C. M. Isborn, S. I. L. Kokkila-Schumacher, X. Li, F. Liu, N. Luehr, J. W. Snyder, C. Song, A. V. Titov, I. S. Ufimtsev, L. P. Wang, T. J. Martínez, *Wiley Interdiscip Rev Comput Mol Sci* **2021**, *11*, DOI 10.1002/wcms.1494.

[46] C. He, Z. Li, Y. Lei, W. Zou, B. Suo, *J Phys Chem Lett* **2019**, *10*, 574–580.

[47] S. Dümmler, W. Roth, I. Fischer, A. Heckmann, C. Lambert, *Chem Phys Lett* **2005**, *408*, 264–268.

[48] A. Heckmann, S. Dümmler, J. Pauli, M. Margraf, J. Köhler, D. Stich, C. Lambert, I. Fischer, U. Resch-Genger, *Journal of Physical Chemistry C* **2009**, *113*, 20958–20966.

[49] E. G. Hohenstein, M. E. F. Bouduban, C. Song, N. Luehr, I. S. Ufimtsev, T. J. Martínez, *J Chem Phys* **2015**, *143*, DOI 10.1063/1.4923259.

[50] P. Slavíček, T. J. Martínez, *J Chem Phys* **2010**, *132*, DOI 10.1063/1.3436501.

[51] F. Weigend, R. Ahlrichs, *Physical Chemistry Chemical Physics* **2005**, *7*, 3297–3305.

[52] K. Eichkorn, O. Treutler, H. Öhm, M. Häser, R. Ahlrichs, *Chem Phys Lett* **1995**, *240*, 283–290.

[53] R. O. Jones, O. Gunnarsson, *Reviews of Modern Physics* **1989**, *61*, 689–746.

[54] J. N. Harvey, *Physical Chemistry Chemical Physics* **2007**, *9*, 331–343.